Electronic Supplementary Material (ESI) for Journal of Materials Chemistry A.

Electronic Supplementary Information (ESI)

“All-in-One” Hypergolic Metal-Organic Frameworks with High Energy Density and Short Ignition Delay

Zhi-Min Li [a*] Yi-Qiang Xu,[a] Chao Wang,[b] Guo-Rong Lei,[a] Rui Zhang,[c] Lei Zhang,[a, c] Jian-Hua Chen,[c] Jian-Guo Zhang,[a] Tong-Lai Zhang[a], Qian-You Wang[b*]

[a] State Key Laboratory of Explosion Science and Technology. Explosion Protection and Emergency Disposal Technology Engineering Research Center of the Ministry of Education. Beijing Institute of Technology. Beijing 100081, China

[b] Henan Key Laboratory of Crystalline Molecular Functional Materials. Green Catalysis Center and College of Chemistry. Zhengzhou University, Zhengzhou 450001, P. R. China

[c] China Science and Technology on Applied Physical Chemistry Laboratory. Shaanxi Applied Physics-Chemistry Research Institute. Xi’an 710061, China

Corresponding authors:

*(Z. M. Li) E-mail: lizm@bit.edu.cn

*(Q. Y. Wang) E-mail: qianyouwang@zzu.edu.cn

Materials and Instrumentations

Caution! The substances used in this work are all hazardous and may explode under certain conditions. Protective equipment, such as face shields, must be worn during experimental operation.

Analytically pure copper nitrate trihydrate and azole ligands were purchased from Shanghai Meirel Chemical Technology Co., Ltd. NaCTB was prepared according to the method reported in literature.[1]

The X-ray diffraction patterns were acquired using a diffractometer operated in multi-scan mode, at the temperature of 153(2) K. The obtained crystallographic data (Table 1) were processed using the SHELXL-2015 and OLEX2 software programs in order to determine the crystal structures. The non-hydrogen atoms were located based on the difference Fourier map, and they were freely refined. The thermal behavior of the MOFs was tested using differential scanning calorimetry (DSC) measurements and thermogravimetric analysis (TGA) conducted in the temperature range of 40–500°C, in air atmosphere, and at heating rates is 10°C·min^{-1}. About 250 mg of MOF sample was placed in a crucible and placed into the oxygen bomb that was filled with enough oxygen for the heat of combustion testing. The powder X-ray diffraction data were collected on a Riguku D/Max-2500PC X-ray diffractometer equipped with a Cu sealed tub (λ = 1.54178 Å). A Phantom VEO710 high-speed charge-coupled device camera was used to capture ignition photos at 1000 frames/s.

Experimental Section

Synthesis procedure

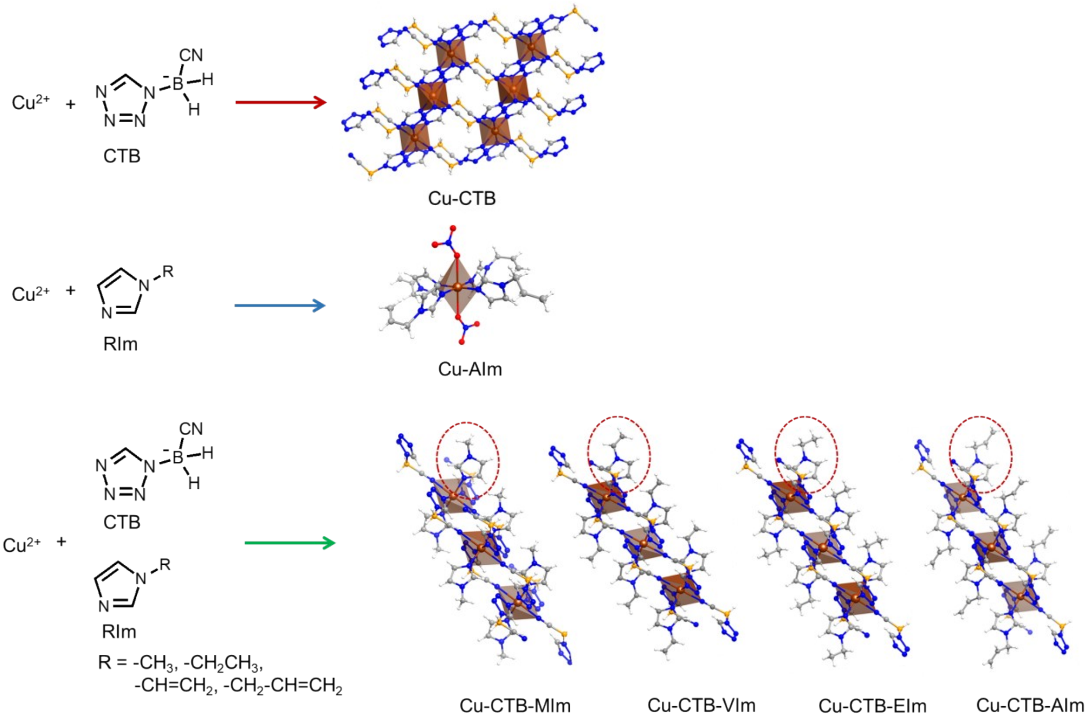

Figure S1. The synthesis routes of Cu-CTB, Cu-AIM and Cu-CTB-RIm.

Synthesis of Cu-CTB-RIm

0.242 g (1 mmol) of copper nitrate trihydrate was added to a round-bottom flask with 20 mL of water, and was stirred at 60 °C until complete dissolution. Then, 0.164 g (2 mmol) of 1-methylimidazole aqueous solution (5 mL) was added to the round-bottom flask, after reacting 30 min, 0.220 g (2 mmol) of NaCTB aqueous solution (5 mL) were slowly added to the mixture, and the reaction was continued for 2 h. Subsequently, the mixture was cooled to room temperature, and the solid product (Cu-CTB-MIm) was collected by filtration and washed with deionized water and ethanol before dried at 60 °C for 6 h.

Cu-CTB-EIm, Cu-CTB-AIm and Cu-CTB-VIm were prepared using a similar procedure to that described for Cu-CTB-MIm, but with different ligands.

Synthesis of Cu-CTB

0.242 g (1 mmol) of copper nitrate trihydrate was added to a round-bottom flask with 10 mL of water, and was stirred at 60 °C until complete dissolution. Then, 0.220 g (2 mmol) of NaCTB aqueous solution (10 mL) was slowly added to the above solution, and the reaction was continued for 2 h. Subsequently, the mixture was cooled to room temperature, and the solid product was collected by filtration and washed with deionized water and ethanol before dried at 60 °C for 6 h.

Synthesis of Cu-AIm

0.242 g (1 mmol) of copper nitrate trihydrate was added to a round-bottom flask with 10 mL of water, and was stirred at 60 °C until complete dissolution. Then, 0.108 g (1 mmol) of 1-Allylimidazole aqueous solution (10 mL) was slowly added to the above solution, and the reaction was continued for 2 h. Subsequently, the mixture was cooled to room temperature, and the solid product was collected by filtration and washed with deionized water and ethanol before dried at 60 °C for 6 h.

FT-IR Characterization of Cu-CTB-RIm

Infrared spectra of the synthesized MOFs were recorded in the spectral range of 400–4000 cm^{-1}, at the resolution of 4 cm^{-1}. MOFs samples were pressed into pellets with KBr. The Fourier transform infrared absorption peaks detected for Cu-CTB-RIm are as follows: Cu-CTB-MIm, IR(KBr): 833, 931, 976, 1017, 1097, 1248, 2226, 2417, 2501, 2557, and 2595 cm^{-1}; Cu-CTB-EIm IR(KBr): 839, 866, 935, 1028, 2153, 2226, 2419, 2498, and 2574 cm^{-1}; Cu-CTB-VIm IR(KBr): 941, 978, 1046, 2207, 2507, 2562, and 2879 cm^{-1}; Cu-CTB-AIm IR(KBr): 931, 1022, 1088, 2227, 2424, 2500, 2551, and 2878 cm^{-1}.

Hypergolic test.

The hypergolic properties of Cu-CTB-RIm, Cu-CTB and Cu-AIm-NO_3 were evaluated by the "oxidizer-fuel" drop test. White fuming nitric acid (WFNA) was used as the oxidant. Each glass vial (5 mL) contained ~15 mg of sample, and a drop of WFNA (30 µL) was added into the vial from a fixed height of 6 cm. Then, the burning process was recorded by a high-speed camera at a speed of 1000 frames per second. IDs were determined by counting the frames between the contact the WFNA with solid materials and the frame first appears.

Calculation of enthalpy of formation($\Delta_f H^\theta m$)

The precise rotating oxygen-bomb calorimeter could measure the constant-volume combustion energy of MOF.[2] The constant-volume combustion energy ($\Delta_c U$) obtained through experiments can be used to calculate the standard molar enthalpies of combustion ($\Delta_c H^\vartheta_m$). The formula used to calculate $\Delta_c H^\vartheta_m$ is $\Delta_c H^\vartheta_m = \Delta_c U^\vartheta_m + [n_g(\text{products}) - n_g(\text{reactants})]RT$, where R = 8.314 $J \cdot mol^{-1} \cdot K^{-1}$, T = 298.15 K, and n_g =total moles of gas in the reaction. The combustion reaction equations of Cu-CTB-RIm are as follows in order:

Equation **1**: $C_{12}H_{18}N_{14}B_2Cu + 18.5\ O_2 \rightarrow CuO(s) + B_2O_3(s) + 12\ CO_2(g) + 9\ H_2O(l) + 7\ N_2(g)$,

Equation **2**: $C_{14}H_{22}N_{14}B_2Cu + 21.5\ O_2 \rightarrow CuO(s) + B_2O_3(s) + 14\ CO_2(g) + 11\ H_2O(l) + 7\ N_2(g)$,

Equation **3**: $C_{14}H_{18}N_{14}B_2Cu + 20.5\ O_2 \rightarrow CuO(s) + B_2O_3(s) + 14\ CO_2(g) + 9\ H_2O(l) + 7\ N_2(g)$,

Equation **4**: $C_{16}H_{22}N_{14}B_2Cu + 23.5\ O_2 \rightarrow CuO(s) + B_2O_3(s) + 16\ CO_2(g) + 11\ H_2O(l) + 7\ N_2(g)$,

The $\Delta_c U$ values of Cu-CTB-RIm obtained in the experiment were −21400 $J \cdot g^{-1}$, −22210 $J \cdot g^{-1}$, −24040 $J \cdot g^{-1}$, and −28990

J·g^{-1}, respectively; thus, the calculated $\Delta_c H^{\vartheta}_m$ could be derived as −9492.8 kJ·mol^{-1}, −10945.1 kJ·mol^{-1}, −11241.1 kJ·mol^{-1}, and −13376.1 kJ·mol^{-1} for **Cu-CTB-MIm**, **Cu-CTB-EIm**, **Cu-CTB-VIm** and **Cu-CTB-AIm**, respectively. Hess's law in thermochemical equations was used to calculate the $\Delta_f H^{\vartheta}_m$. For example, $\Delta_f H^{\vartheta}_m$ (Cu-CTB-MIm) = $\Delta_f H^{\vartheta}_m$ (CuO, s) +$\Delta_f H^{\vartheta}_m$ (B_2O_3, s) + 12$\Delta_f H^{\vartheta}_m$ (CO_2, g) + 9$\Delta_f H^{\vartheta}_m$ (H_2O, l) − $\Delta_c H^{\vartheta}_m$ (Cu-CTB-MIm). $\Delta_f H^{\vartheta}_m$ (CO_2, g) = −393.51 kJ·mol^{-1}, $\Delta_f H^{\vartheta}_m$ (CuO, s) = −155.20 kJ·mol^{-1}, $\Delta_f H^{\vartheta}_m$ (B_2O_3, s) = −1271.94 kJ·mol^{-1}, and $\Delta_f H^{\vartheta}_m$ (H_2O, l) = −285.83 kJ·mol^{-1} were obtained from the standard mole formation enthalpy table and the literature.[3, 4] The calculated $\Delta_f H^{\vartheta}_m$ of **Cu-CTB-MIm**, **Cu-CTB-EIm**, **Cu-CTB-VIm** and **Cu-CTB-AIm** are 771.05, 864.65, 1732.39, and 2508.65 kJ·mol^{-1}, respectively.

Calculation of specific impulse (I_{sp})

The program of Chemical Equilibrium with Applications,[5, 6] developed by NASA researchers, was used to calculate the specific impulse of MOF, according to the formula $I_{sp} = k\sqrt{Tc/M}$, I_{sp} is related to the gaseous combustion temperature (T_c) and the average molecular mass of the combustion gas (M). In the entire calculation, the following are considered: ambient temperature = 298.15 K, fuel-to-oxidizer ratio = 2.0–5.0, P_c = 25 atm, P_e = 1 atm, A_e/A_t = 4, and freezing flow conditions during expansion.[7] The oxidant is WFNA, which is consistent with the oxidant used in the subsequent hypergolic test.

Theoretical Calculations

The density of states (DOS) and electrostatic potential (ESP) on the molecular van der Waals (vdW) surface were determined with the Vienna Ab initio Software Package (VASP 5.3.5) code under the Perdew–Burke–Ernzerhof (PBE) generalized gradient approximation and the projected augmented wave (PAW) method. The cut-off energy for the plane-wave basis set was set to 400 eV. The Brillouin zone of the surface unit cell was sampled by Monkhorst–Pack (MP) grids for structure optimizations.

Supplemental Figures and Tables

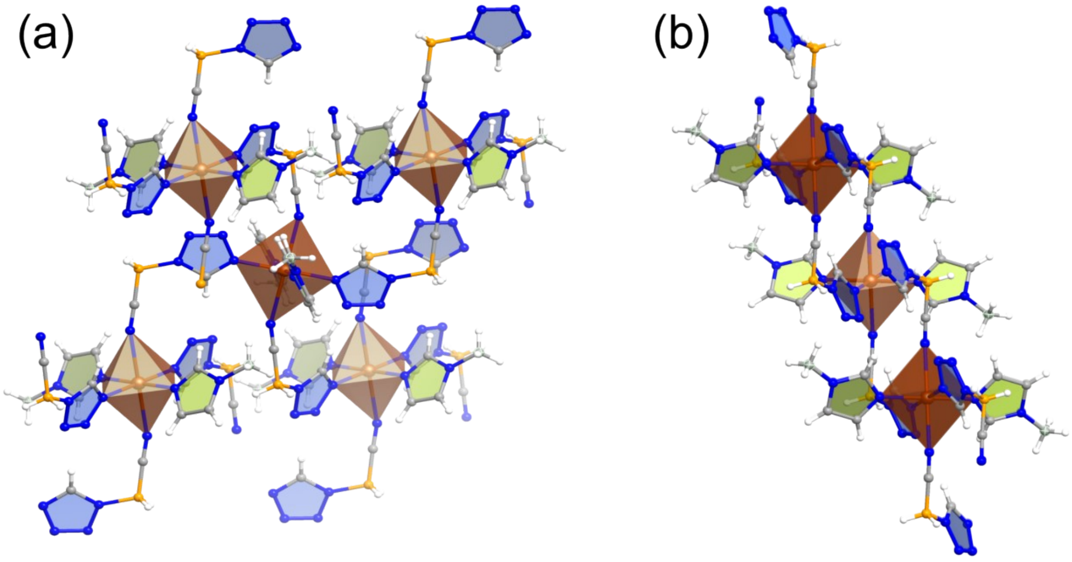

Figure S2. Crystal structure of Cu-CTB-MIm.

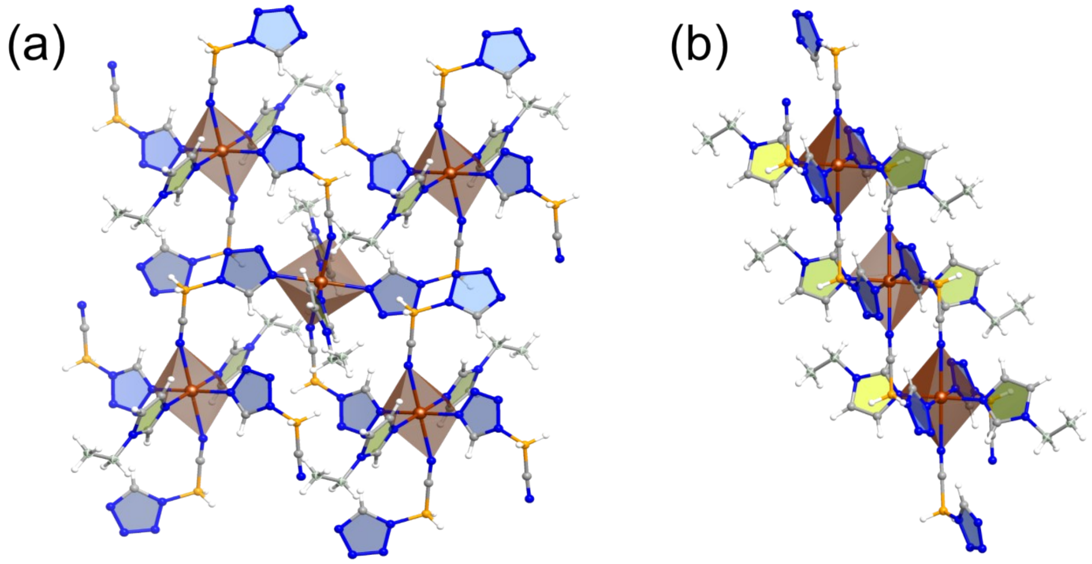

Figure S3. Crystal structure of Cu-CTB-VIm.

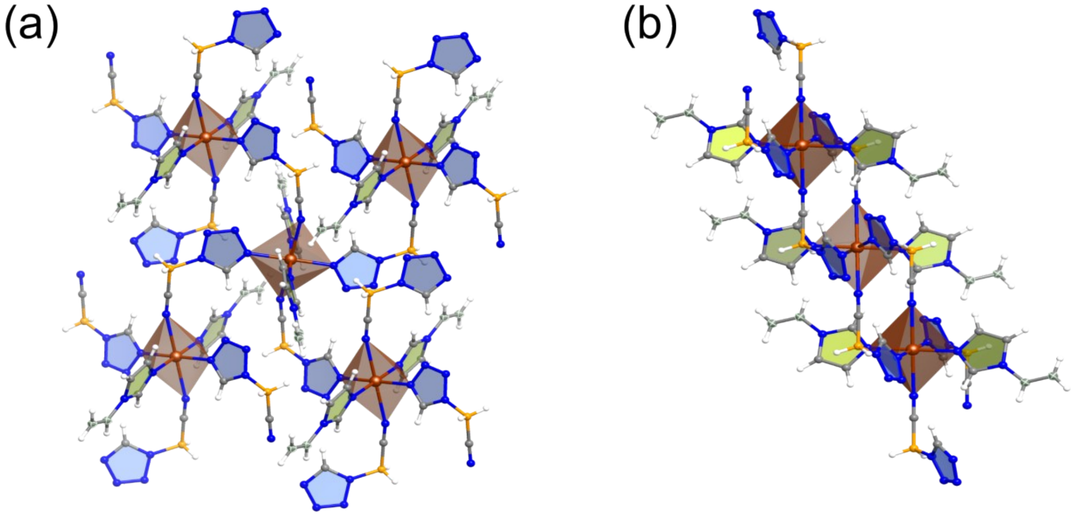

Figure S4. Crystal structure of Cu-CTB-EIm.

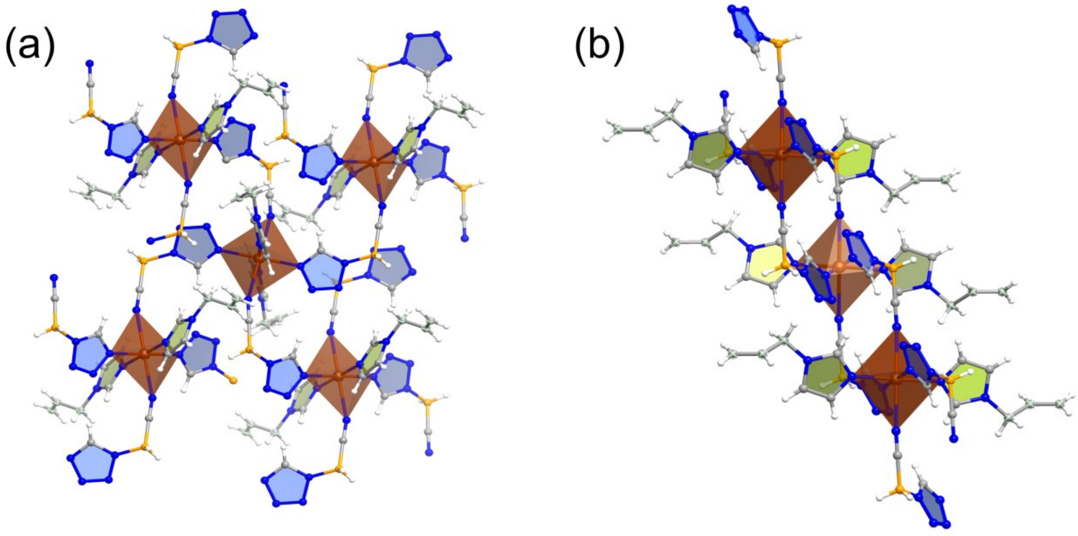

Figure S5. Crystal structure of Cu-CTB-AIm.

Table S1. X-ray crystallographic data corresponding toCu-CTB-RIm, Cu-CTB and Cu-AIm.

	Cu-CTB-MIm	**Cu-CTB-EIm**	**Cu-CTB-AIm**	**Cu-CTB-VIm**	**Cu-CTB**	**Cu-AIm**
Empirical formula	$C_{12}H_{18}N_{14}B_2$ Cu	$C_{14}H_{22}N_{14}B_2$ Cu	$C_{16}H_{22}N_{14}B_2$ Cu	$C_{14}H_{18}B_2N_{14}$ Cu	$C_{12}H_{18}B_6N_{30}$ Cu_3	$C_{24}H_{32}O_6N_{10}$ Cu
Crystal system	Monoclinic	Monoclinic	Monoclinic	Monoclinic	Monoclinic	Triclinic
Space group	$P2_1$/n	$P2_1$/n	$P2_1$/c	$P2_1$/c	$P2_1$/c	*P-1*
Density (g·cm^{-3})	1.448	1.530	1.455	1.537	1.700	1.524
a/Å	10.2506(9)	10.5143(9)	10.9096(11)	10.5342(12)	21.194(2)	8.8723(11)
b/Å	10.1588(11)	9.8449(8)	9.7192(9)	9.6428(11)	8.5850(8)	8.9291(10)
c/Å	10.8037(11)	11.0882(9)	11.5319(13)	11.0538(13)	9.0509(9)	9.0178(12)
α/(°)	90.00	90.00	90.00	90.00	90.00	105.573(11)
β/(°)	115.301(4)	116.865(4)	112.316(5)	115.872(4)	96.100(2)	98.353(11)
γ/(°)	90.00	90.00	90.00	90.00	90.00	94.530(10)
Volume/nm^3	1017.11(18)	1023.89(15)	1131.2(2)	1010.3(2)	1637.5(3)	675.64(14)
Z	2	2	2	2	2	1
μ/ mm^{-1}	1.104	1.102	1.667	1.116	1.993	0.868
F(000)	454.0	486.0	510.0	478.0	834.0	323.0
Crystal size/mm^3	0.3 × 0.11 × 0.1	0.3 × 0.1 × 0.08	0.2 × 0.06 × 0.04	0.4 × 03 × 0.11	0.11 × 0.10 × 0.05	0.33 × 0.33 × 0.16
2θ range/(°)	4.58° to 50.04°	4.44° to 50.04°	8.76° to 132.02°	5.88° to 50.02°	3.86° to 50.02°	7.08° to 51.98°
Reflections collected	4940	4779	1970	4919	2873	4305
Independent reflections	1785[R_{int} = 0.1138, R_{sigma}=0.0889]	1796[R_{int}= 0.1287, R_{sigma}=0.1149]	1970[R_{int}= 0.0000, R_{sigma}=0.0902]	1783[R_{int} = 0.0396, R_{sigma}=0.1680]	2873[R_{int} = 0.0000, R_{sigma}=0.1680]	2570[R_{int}= 0.0390, R_{sigma}=0.0707]
Goodness-of-fit on F^2	1.063	1.046	1.112	1.037	1.033	1.086
Final R indices($I > 2\sigma(I)$)	R_1 = 0.0654, wR_2 = 0.1616	R_1 = 0.0668, wR_2 = 0.1504	R_1 = 0.0680, wR_2 = 0.1582	R_1 = 0.0373, wR_2 = 0.0974	R_1 = 0.0841, wR_2 = 0.1689	R_1 = 0.0431, wR_2 = 0.0930
R indices (all data)	R_1 = 0.0867, wR_2 = 0.1742	R_1 = 0.0976, wR_2 = 0.1634	R_1 = 0.0971, wR_2 = 0.1731	R_1 = 0.0455, wR_2 = 0.1010	R_1 = 0.2060, wR_2 = 0.2289	R_1 = 0.0495, wR_2 = 0.0996
CDCC	2059562	2059564	2059563	2094480	2087483	2111636

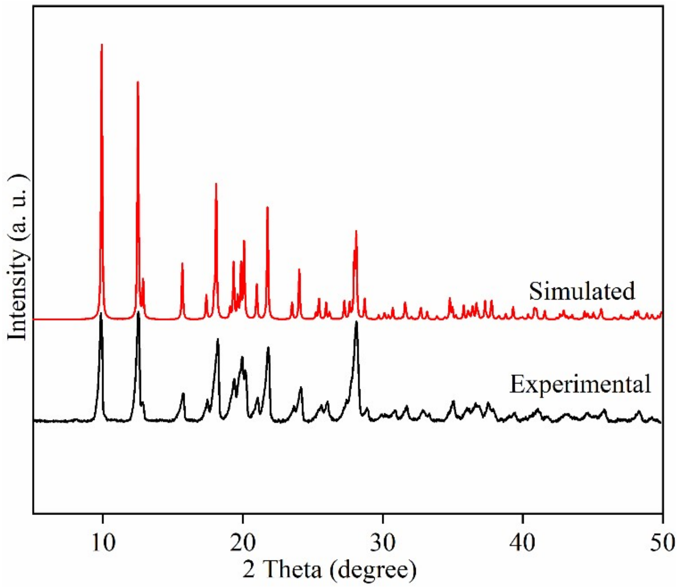

Figure S6. Powder X-ray diffraction patterns for the experimental and simulated Cu-CTB-MIm.

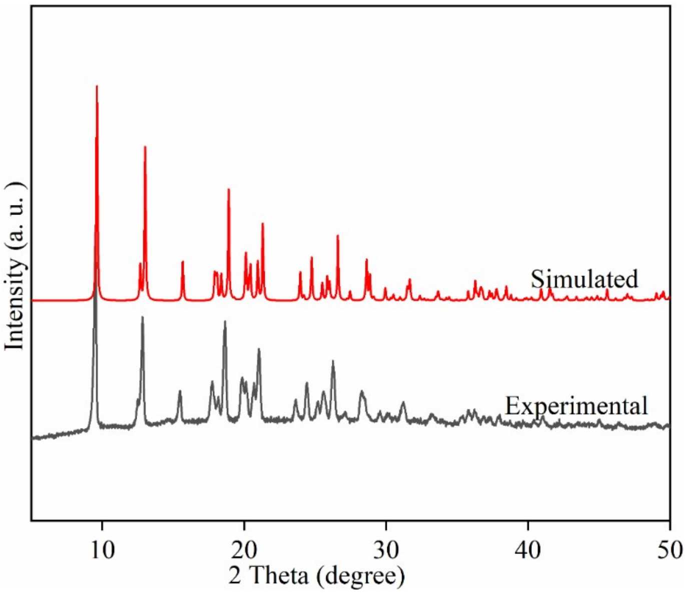

Figure S7. Powder X-ray diffraction patterns for the experimental and simulated Cu-CTB-EIm.

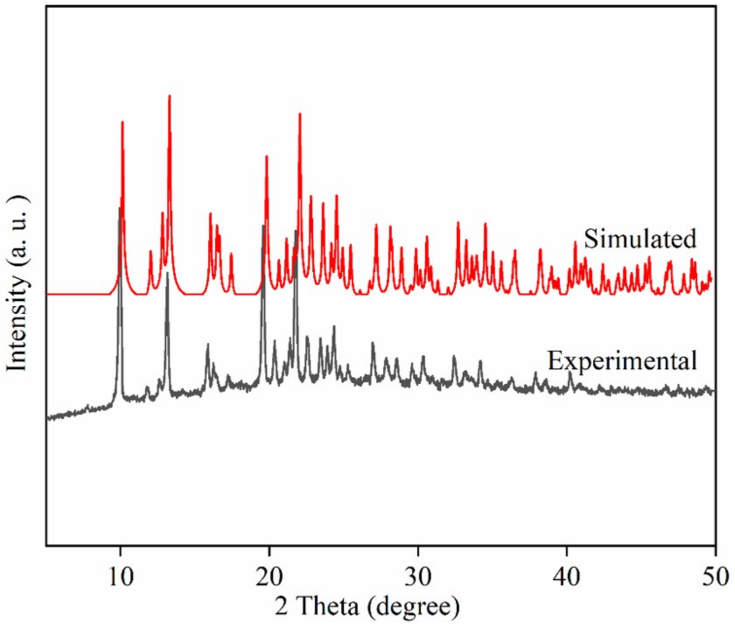

Figure S8. Powder X-ray diffraction patterns for the experimental and simulated Cu-CTB-AIm.

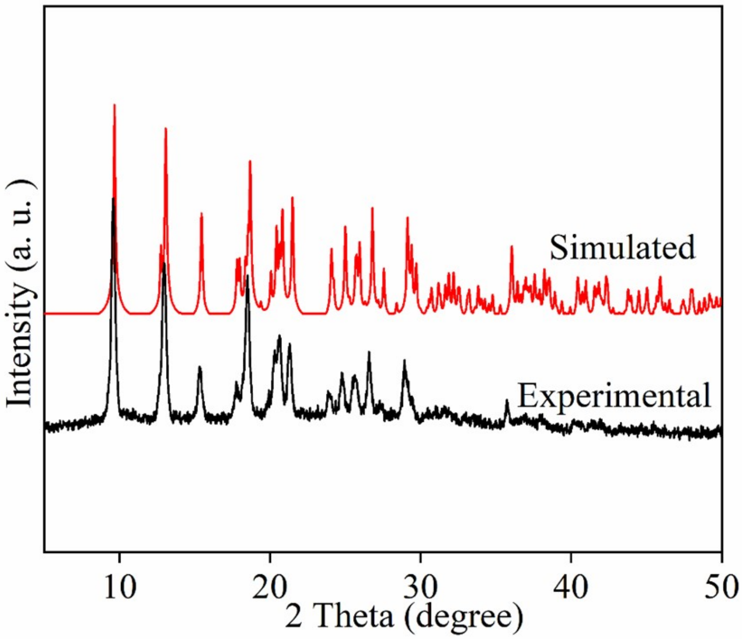

Figure S9. Powder X-ray diffraction patterns for the experimental and simulated Cu-CTB-VIm .

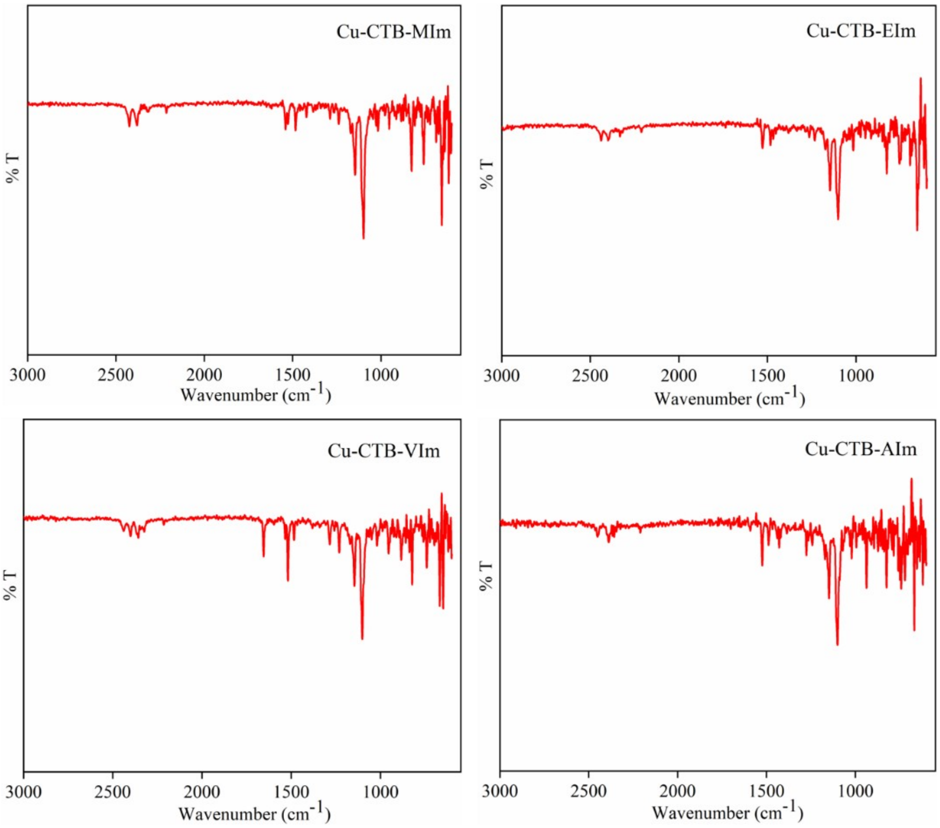

Figure S10. The FT-IR spectra of Cu-CTB-MIm, Cu-CTB-EIm, Cu-CTB-VIm and Cu-CTB-AIm, respectively.

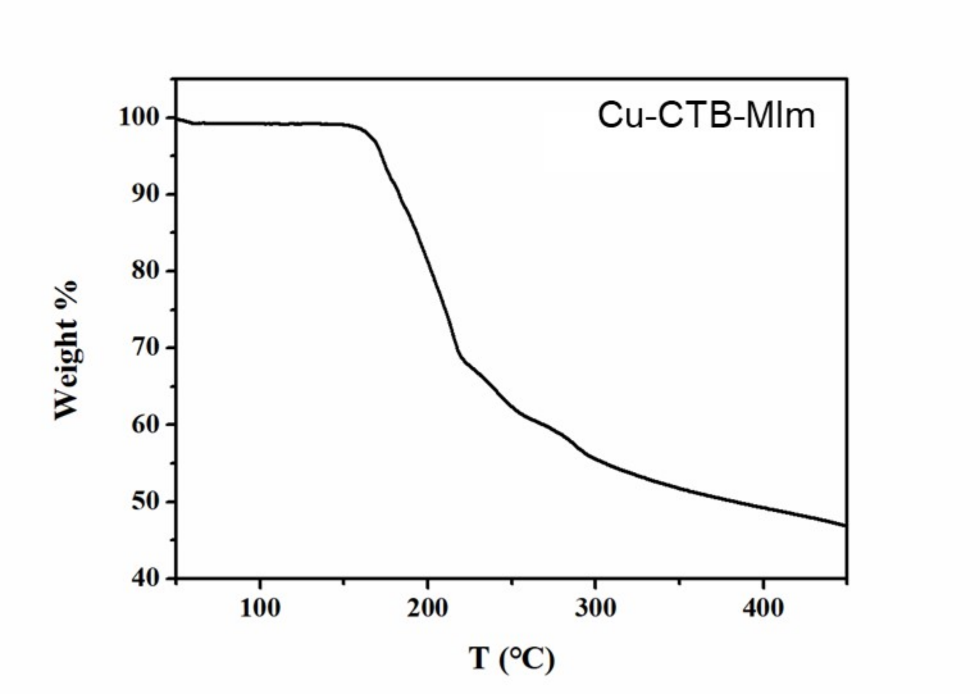

Figure S11. Thermogravimetry curve of Cu-CTB-MIm.

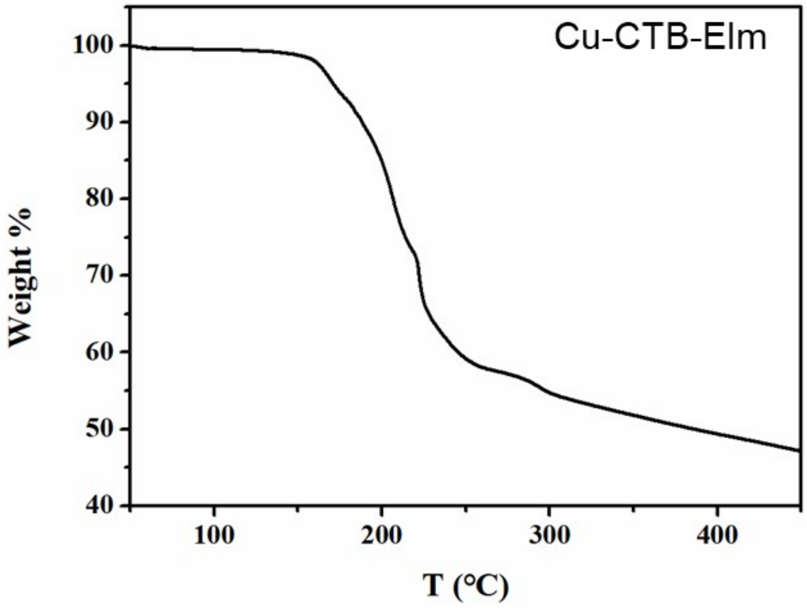

Figure S12. Thermogravimetry curve of Cu-CTB-EIm.

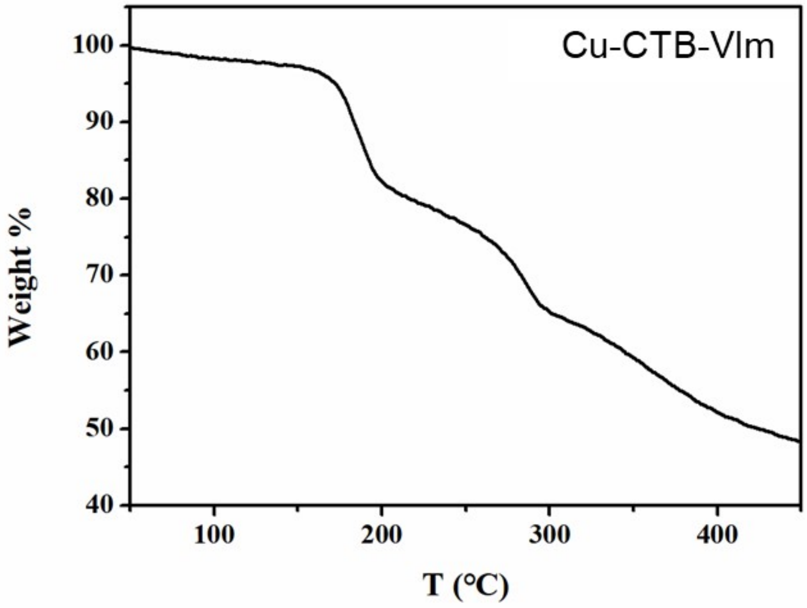

Figure S13. Thermogravimetry curve of Cu-CTB-VIm.

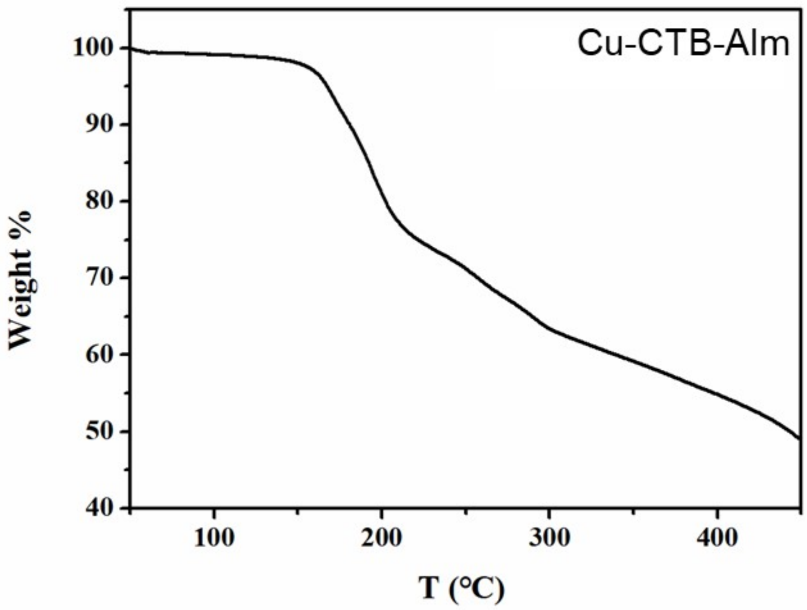

Figure S14. Thermogravimetry curve of Cu-CTB-AIm.

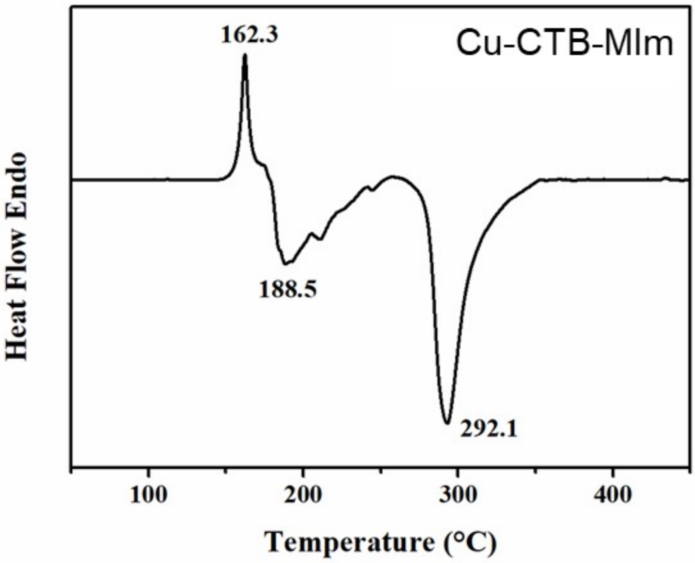

Figure S15. The DSC curve of Cu-CTB-MIm.

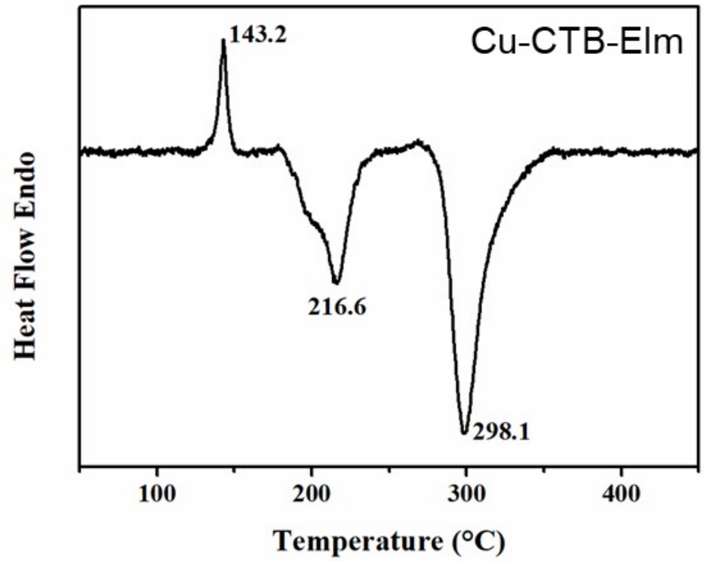

Figure S16. The DSC curve of Cu-CTB-EIm.

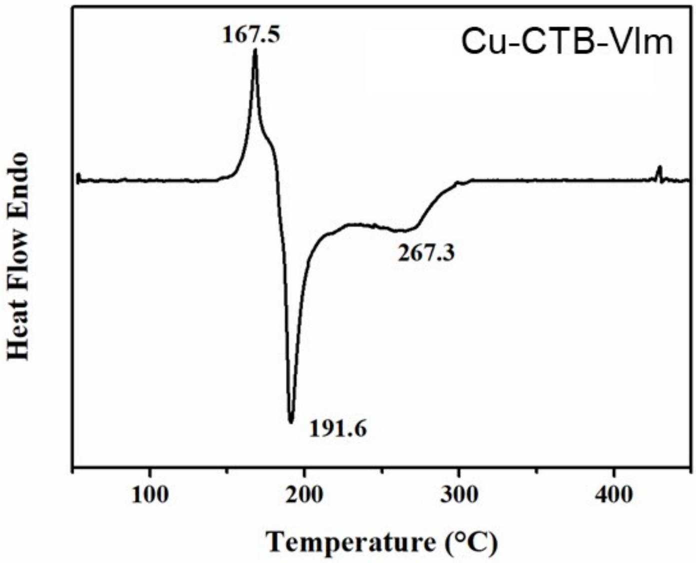

Figure S17. The DSC curve of Cu-CTB-Vim.

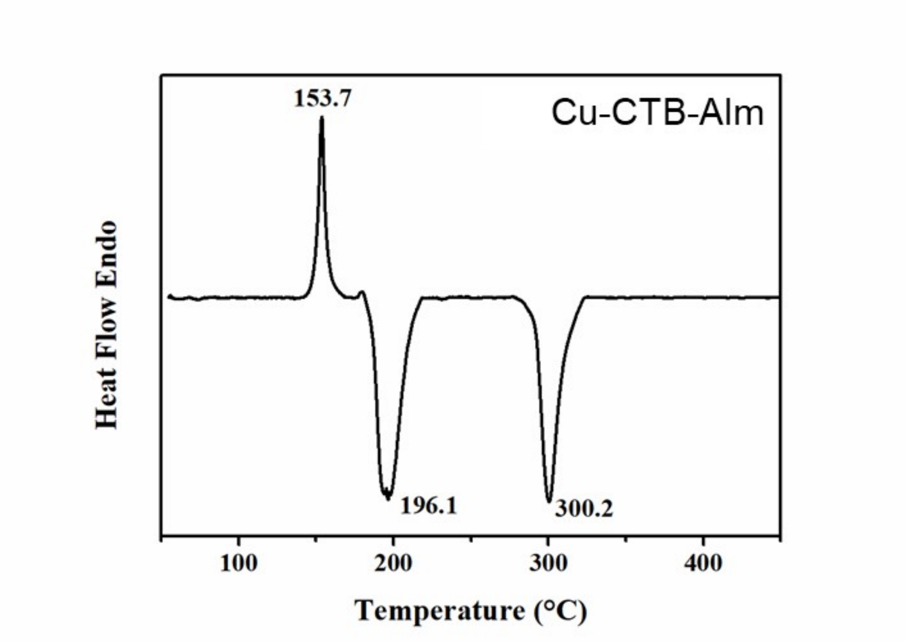

Figure S18. The DSC curves of Cu-CTB-AIm.

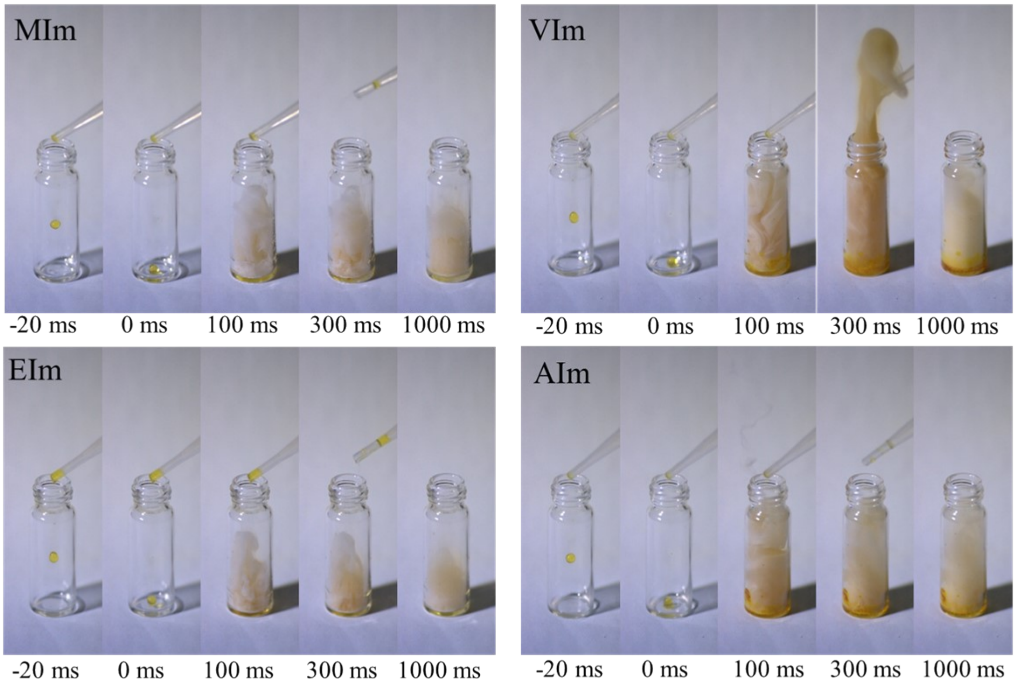

Figure S19. Hypergolicity drop tests for pure imidazole ligands.

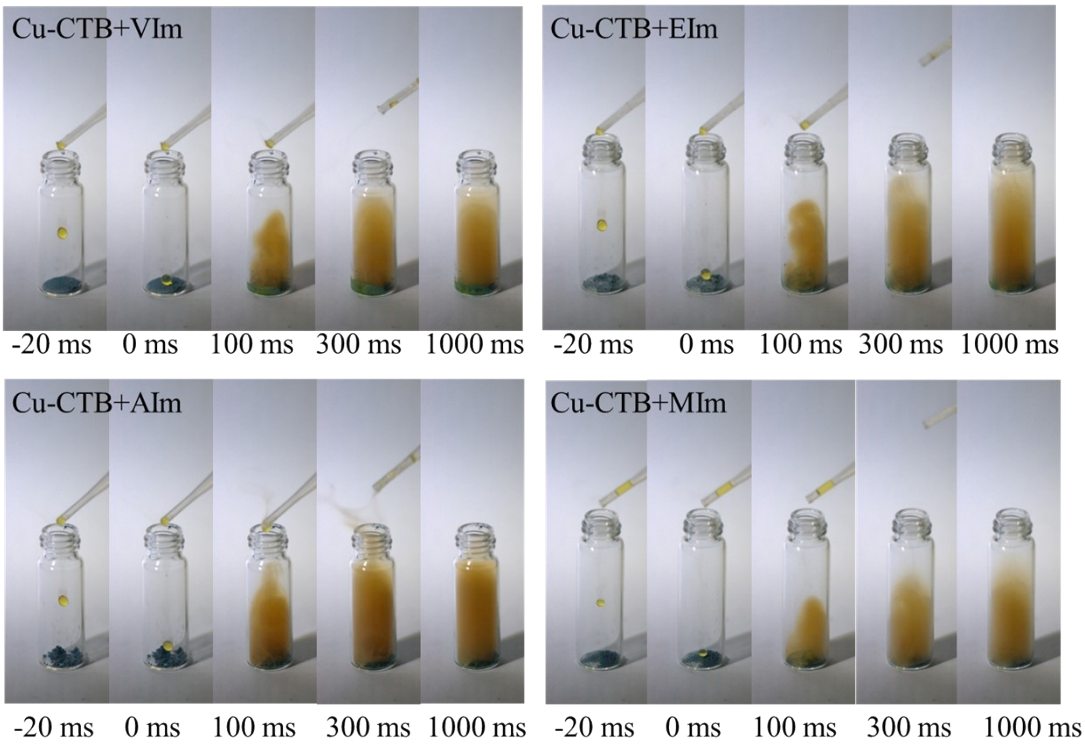

Figure S20. Hypergolicity drop tests for the mixtures of Cu-CTB and Rim ligands.

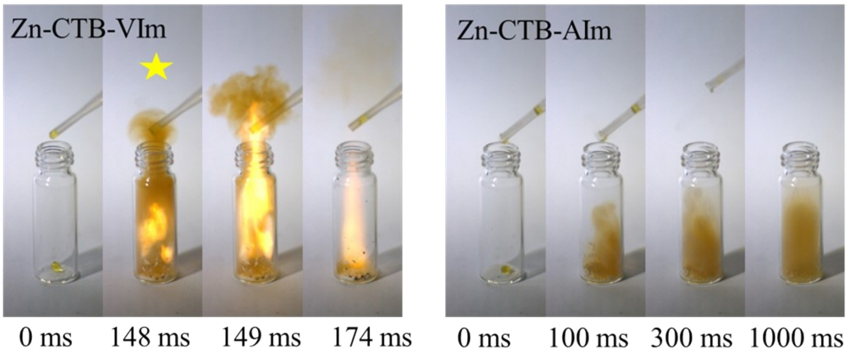

Figure S21. Hypergolicity drop tests for the Zn-CTB-VIm and Zn-CTB-AIm, respectively.

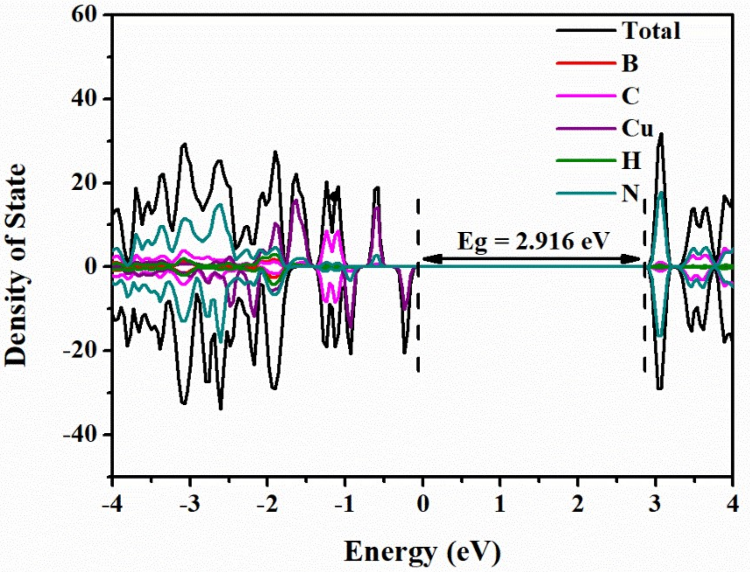

Figure 22. Total and partial density of states (DOS) of Cu-CTB-MIm**.**

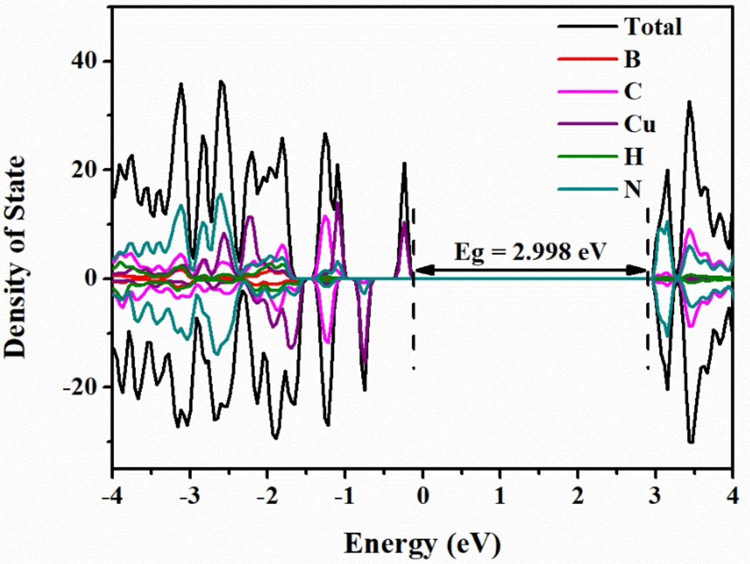

Figure S23. Total and partial density of states (DOS) of Cu-CTB-AIm**.**

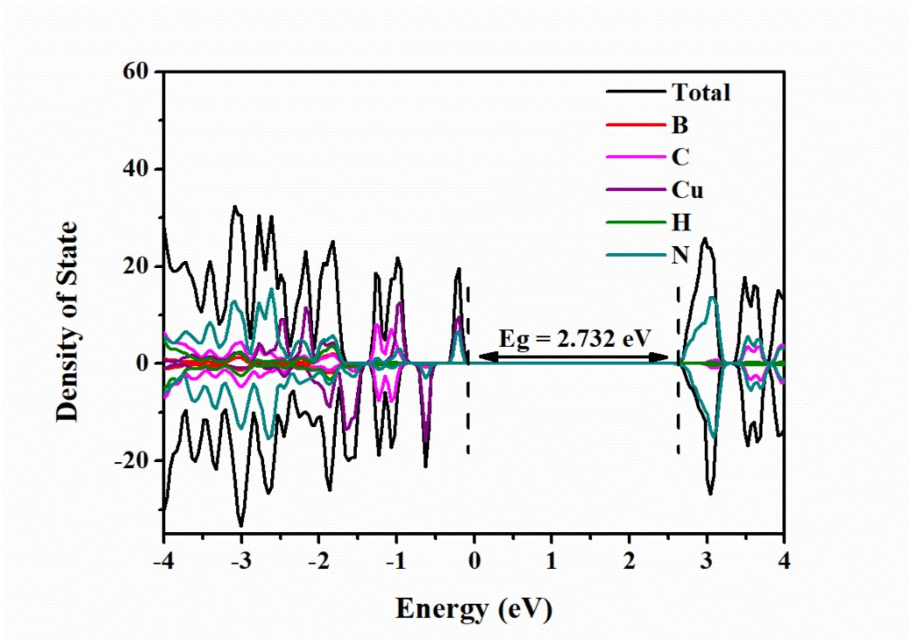

Figure S24. Total and partial density of states (DOS) of Cu-CTB-EIm.

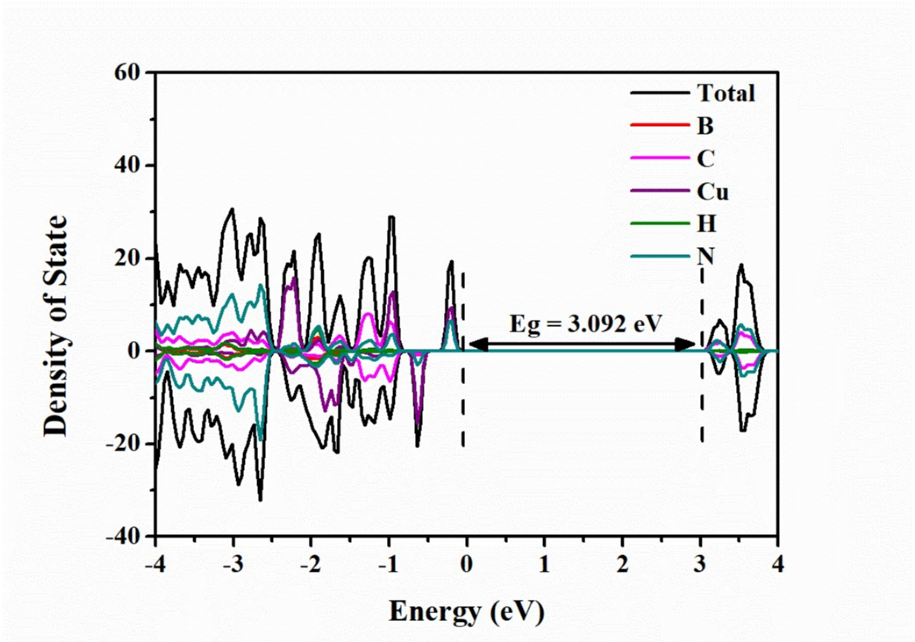

Figure S25. Total and partial density of states (DOS) of Cu-CTB-VIm.

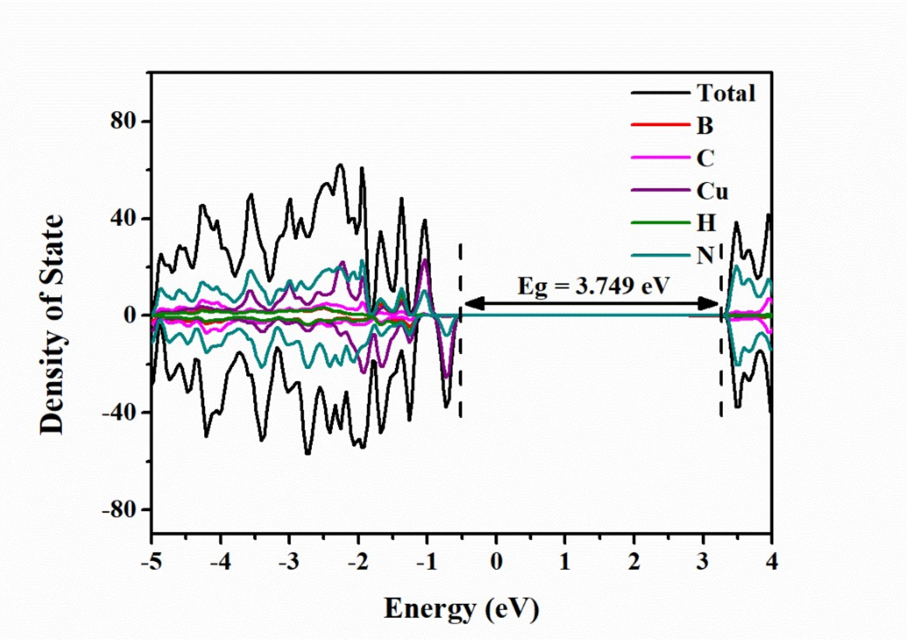

Figure S26. Total and partial density of states (DOS) of Cu-CTB.

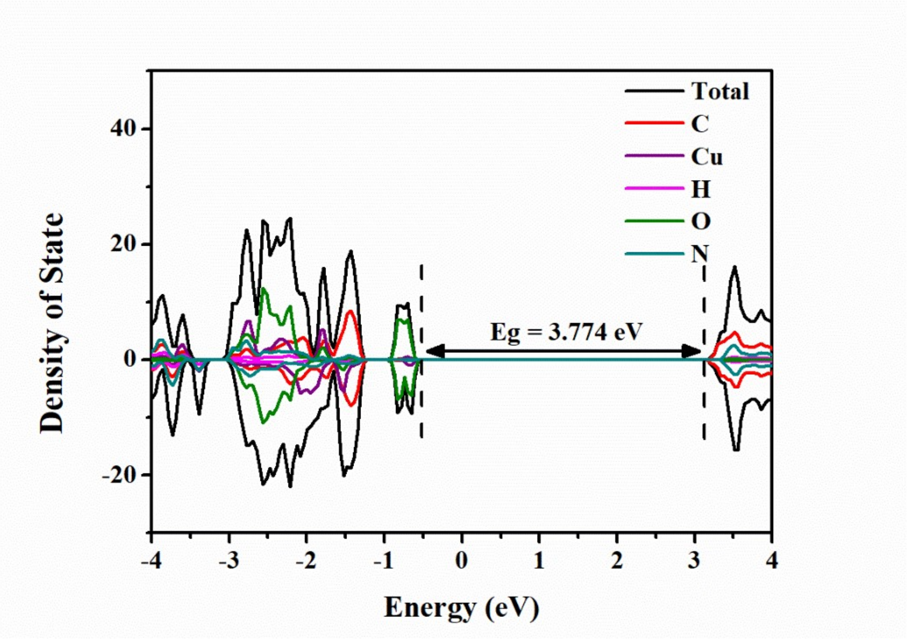

Figure S27. Total and partial density of states (DOS) of Cu-AIm.

Notes and references

1. X. Li, H. Huo, H. Li, F. Nie, H. Yin, F. X. Chen, *Chem. Commun.*, 2017, **53**, 8300-8303.
2. X. W. Yang, S. P. Chen, S. L. Gao, H. Y. Li, Q. Z. Shi, *Instrum. Sci. Technol.,* 2002, **30**, 311-321.
3. N. A. Mayer, D. M. Cupid, R. Adam, A. Reif, D. Rafaja, H. J. Seifert, *Thermochim*. *Acta.,* 2017, **652**, 109-118.
4. K. T. Jacob, A. Kumar, G. Rajitha, Y. Waseda, *High Temp. Mater. Processes.,* 2011, **30**, 459-472.
5. B. J. McBride, S. Gordon, I. Analysis. II. Users Manual and Program Description 1994, (PART 1).
6. B. J. McBride, M. J. Zehe, S. Gordon, Thermodynamic Properties of Individual Species. 2002.
7. V. K. Bhosale, J. Jeong, J. Choi, D. G. Churchill, Y. Lee, S. Kwon, *Combust. Flame* 2020, **214**, 426-436.